



	<b>Experiment title:</b> Spatial distribution of magnesium around biodegradable implants	<b>Experiment number:</b> MA 3043
<b>Beamline:</b> ID 20	<b>Date of experiment:</b> from: 4.6.2017 to: 7.6.2017	<b>Date of report:</b> 31.5.2017  <i>Received at ESRF:</i>
<b>Shifts:</b> 9	<b>Local contact(s):</b> Christoph Sahle	
<b>Names and affiliations of applicants</b> (* indicates experimentalists): D.C.F. Wieland*, Helmholtz Zentrum Geesthacht, Max-Planck-Straße 1, 22761 Geesthacht Silvia Galli*, Laboratory Faculty of Odontology Malmö Univeristy Carl Gustavs Väg 34 SE - 20506 MALMO Christoph Sahle*, Laboratory ESRF 71 avenue des Martyrs CS 40220 FR - 38043 Grenoble Cedex 9 Imke Greving*, Helmholtz Zentrum Geesthacht, Max-Planck-Straße 1, 22761 Geesthacht Regine Willumeit-Römer , Helmholtz Zentrum Geesthacht, Max-Planck-Straße 1, 22761 Geesthacht		

### Report:

We investigated the magnesium distribution around biodegradable model implants made of magnesium alloys studied by a tomography approach which is based on x-ray Raman scattering (XRS). Magnesium is thought to be a good candidate for biodegradable implants but its incorporation into bone and its degradation process are not fully understood. Histological studies showed that the bone formation is altered in the surrounding of a magnesium implant. [1, 2] For a better understanding of the corrosion process and a knowledge based development of magnesium implants, the distribution and chemical state of magnesium in the bone matrix is of great interest. In conventional elemental analysis investigations, the specimen has to be cut in slices for investigations because of the low x-ray energies. [1] This drawback can be overcome by direct tomography (DT). [4] By connecting the elemental distribution gained from DT with high resolution  $\mu$ CT measurements of the same specimen a better understanding of the mechanism will be gained, as the magnesium distribution and oxidation state can be directly connected to the structural changes in the bone matrix.

For the measurements we used critical point dried samples of a piece of rat femur with an embedded magnesium implant. The bioresorbable screw was made of the magnesium alloy Mg10Gd. The investigated healing period was 12 weeks. Measurements were performed at

the ID20 with an energy of 10keV and 13keV in order to test which energy was better suitable to maximise the signal with respect to absorption, energy resolution and scan-time. From the measurements it turned out that an energy of 13keV was most suitable as the penetration depth was increased and absorption was reduced. The measurements were performed at the elastic line as well as around the magnesium L-edge. Further the super resolution algorithm was applied on the data, which increased the counts due to combining the different detectors and enables us to reduce the scanning time in further experiments. [5] Figure 1 shows the intensity of the elastic line with a resolution of 50 $\mu$ m along with a conventional  $\mu$ CT image collected on tomography lab source of the sample. A good correspondence between the samples can be seen.

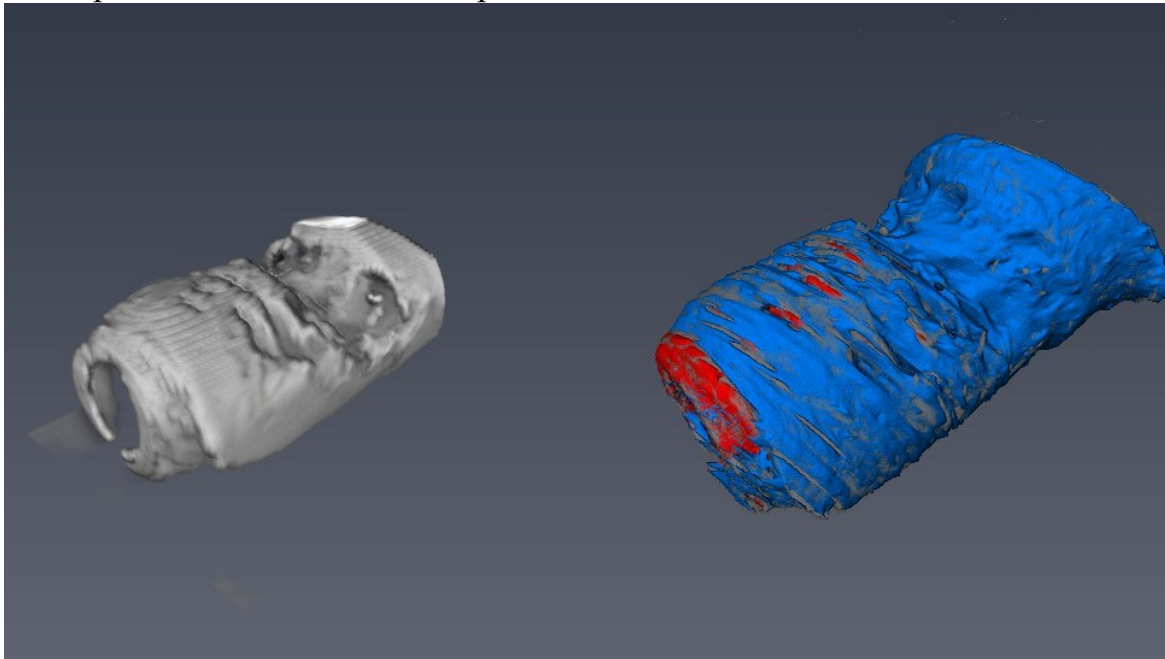


Figure 1: Left. Three dimensional distribution of the signal from the elastic line. Right.: Segmented tomogram from the sample. The Mg Screw (red) and Bone (blue) are segmented for better visibility.

As the sample was quite large 4mm x 4mm x 6 mm, not the complete sample was scanned with highest resolution. Only a small local area of the size 500  $\mu$ m x 500 $\mu$ m was scanned with the highest resolution resulting in a voxel size of 10 $\mu$ m x 10 $\mu$ m x 1  $\mu$ m. Figure 3 shows this high resolution scan of the implant sample in grey colours.

Figure 2 shows the Magnesium L-edge of the bone sample at 49eV which was chosen to perform our studies. The spectra show a very well defined white line and, thus, offers the opportunity for the chemical bond contrast.

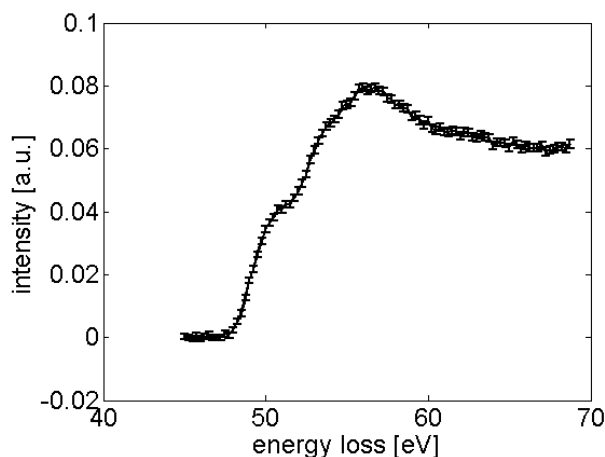


Figure 2 Magnesium L-edge measured in the bone sample with the Mg5Gd screw.

For this, scans before and at the magnesium L-edge were taken. The difference between them was calculated and used as a contrast. Figure 3 shows this contrast difference of the edge along with the high resolution scan.

From this figure the magnesium distribution in the bone can be nicely seen. And it shows the feasibility of the technique to study the Mg

From this figure the magnesium distribution in the

bone can be nicely seen. And it shows the feasibility of the technique to study the Mg

distribution in bone samples. However, some further analysis and data treatment has to be performed in order to make qualitative statements about the Mg distribution. In the ongoing data analysis two major points have still to be considered. First the dataset has to be accounted for absorption and second the  $\mu$ CT image and the XRS-image have to be overlaid to draw combined conclusions from the chemical and structural information. For this both datasets will be registered and spatially correlated. Here problems still exist due to the different spatial resolution of the sample and due to the incompleteness of the XRS-image (shadowing of the backpart). After this is accomplished, also the data can be corrected for absorption. Here we will use the  $\mu$ CT data and the information from the elastic line as both datasets contain equal information with respect to the density of the material.

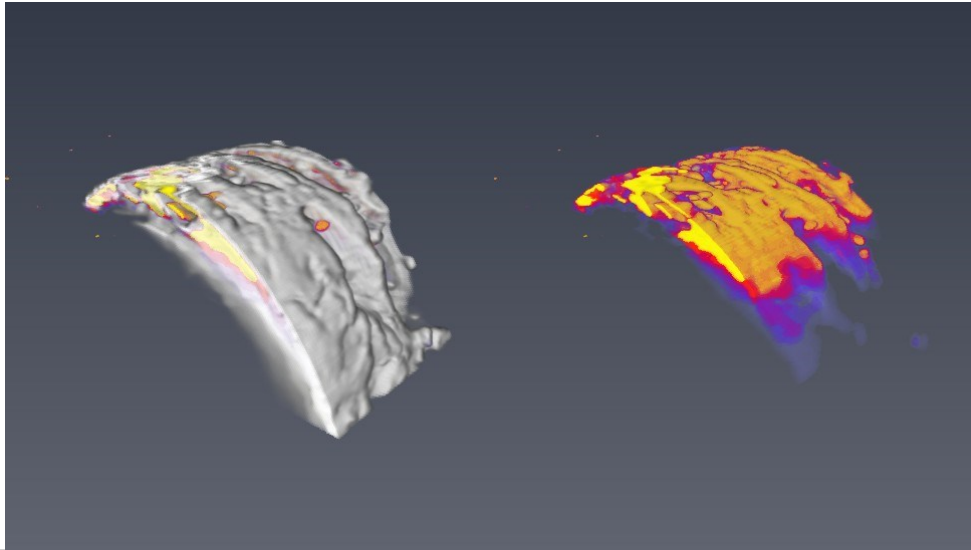


Figure 3, Left) High resolution scan of a part of the implant with bone. Right) Difference of the pre-edge and post-edge, which is also overlaid in the left image.

1. Witte, F., et al., *In vivo corrosion of four magnesium alloys and the associated bone response*. *Biomaterials*, 2005. **26**(17): p. 3557-3563.
2. Witte, F., et al., *Biodegradable magnesium scaffolds: Part II: Peri-implant bone remodeling*. *Journal of Biomedical Materials Research Part A*, 2007. **81A**(3): p. 757-765.
3. Reifenrath, J. et al. *Magnesium alloys as promising degradable implant materials in orthopedic research*, *Magnesium Alloys Corrosion and Surface Treatments*, 2011, p. 93 -108
4. Huotari, S. Direct tomography with chemical-bond contrast, *Nature*, 2011, **10**, p. 489-493
5. Sahle, Ch J., et al., "Improving the spatial and statistical accuracy in X-ray Raman scattering based direct tomography." *Journal of Synchrotron Radiation* **24**, no. 2 (2017): 476-481.